Hydrogen Evolution Hot Paper

International Edition: DOI: 10.1002/anie.201508715
German Edition: DOI: 10.1002/ange.201508715

Hierarchical β-Mo_2C Nanotubes Organized by Ultrathin Nanosheets as a Highly Efficient Electrocatalyst for Hydrogen Production

*Fei-Xiang Ma, Hao Bin Wu, Bao Yu Xia, Cheng-Yan Xu, and Xiong Wen (David) Lou**

Abstract: *Production of hydrogen by electrochemical water splitting has been hindered by the high cost of precious metal catalysts, such as Pt, for the hydrogen evolution reaction (HER). In this work, novel hierarchical β-Mo_2C nanotubes constructed from porous nanosheets have been fabricated and investigated as a high-performance and low-cost electrocatalyst for HER. An unusual template-engaged strategy has been utilized to controllably synthesize Mo-polydopamine nanotubes, which are further converted into hierarchical β-Mo_2C nanotubes by direct carburization at high temperature. Benefitting from several structural advantages including ultrafine primary nanocrystallites, large exposed surface, fast charge transfer, and unique tubular structure, the as-prepared hierarchical β-Mo_2C nanotubes exhibit excellent electrocatalytic performance for HER with small overpotential in both acidic and basic conditions, as well as remarkable stability.*

Hydrogen, as a clean and renewable energy source, has been intensely investigated as a possible alternative to conventional fossil fuels.[1–3] A promising way to produce hydrogen is to electrochemically split water into hydrogen and oxygen gases, driven by highly efficient electrochemical catalysts at low overpotentials.[4,5] Generally, precious Pt-group metals are considered as the most active hydrogen evolution reaction (HER) electrocatalysts, but their scarcity and high cost seriously hinder the scale-up deployment.[6,7] These limitations have motivated intensive efforts to design and fabricate inexpensive and earth-abundant HER electrocatalysts with high catalytic activities.[8–19]

Molybdenum carbide, an important member of early transition-metal carbides, has aroused ever-growing interest as a high-performance HER electrocatalyst because its electronic structure is similar to that of Pt-group metals.[20,21] As a high melting point compound, synthesis of highly crystallized molybdenum carbides generally involves high-temperature pyrolysis of precursors containing molybdenum and carbon/organic compounds. However, high-temperature annealing would often lead to excess growth and coarsening of molybdenum carbide crystallites, which undoubtedly results in low specific surface area and subsequently low density of catalytic active sites. Most of the reported molybdenum carbide nanomaterials and their hybrids are irregular in shape, and very limited research progress has been made in the synthesis of well-defined molybdenum carbide nanostructures with small crystalline size and high porosity.[21–23] For instance, nanoporous β-Mo_2C nanowires and MoC_x nano-octahedrons were recently prepared by direct pyrolysis of a MoO_x/amine hybrid precursor[22] and from metal-organic frameworks (MOFs) containing molybdenum-based polyoxometalates (NENU-5),[23] respectively. Despite these advances, the controllable synthesis of molybdenum carbide nanomaterials with well-defined nanostructures is still highly challenging, mainly because of the lack of proper precursors incorporating uniformly hybridized Mo and carbon sources in well-organized nanostructures.

Dopamine, a representative catechol derivative containing both catechol functions and amino functional groups, has stimulated extensive research as it can easily self-polymerize under alkaline conditions ($pH > 7.5$) to form polydopamine.[24–26] Besides, dopamine shows a strong complexation ability with various ions, including transition-metal ions and metal-containing oxyanions (WO_4^{2-}, MoO_4^{2-} etc.).[24] A representative case is the formation of Mo-dopamine complex based on the interaction between MoO_4^{2-} and catechol groups.[27,28] Thus, composite materials based on strongly coupled Mo and polydopamine (donated as Mo-polydopamine hybrid) could be generated by the oxidative self-polymerization of the Mo-dopamine complex, which might serve as an appealing precursor for nanostructured molybdenum carbides.

Herein, we have rationally designed and synthesized novel hierarchical β-Mo_2C nanotubes constructed from porous nanosheets by carburizing Mo-polydopamine nanotubes under a N_2 gas flow. The two-dimensional (2D) ultrathin nanosheets are expected to expose more active sites than other nanostructures.[29–31] More importantly, by assembling the 2D nanosheets into a well-organized hierarchical hollow architecture, the possibility to lose effective surface as a result of overlapping and aggregation would be minimized.[32–34] Additionally, the robust hierarchical architecture might also facilitate the charge/mass transport in the materials during the electrochemical process. By virtue of the above-mentioned merits, the as-prepared hierarchical tubular structures assembled from 2D ultrathin nanosheets exhibit a large exposed surface, short diffusion distance, and abundant electron/ion transport pathways, which effectively boost the electrocatalytic activity. As a result, these hierarchical β-Mo_2C nanotubes

[*] F. X. Ma, Dr. H. B. Wu, Dr. B. Y. Xia, Prof. X. W. Lou
School of Chemical and Biomedical Engineering
Nanyang Technological University
62 Nanyang Drive, Singapore, 637459 (Singapore)
E-mail: xwlou@ntu.edu.sg
Homepage: http://www.ntu.edu.sg/home/xwlou/
F. X. Ma, Prof. C. Y. Xu
School of Materials Science and Engineering, Harbin Institute of Technology
Harbin, 150001 (China)

Supporting information for this article is available on the WWW under http://dx.doi.org/10.1002/anie.201508715.

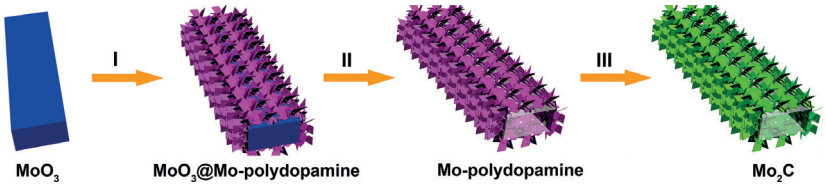

Figure 1. Schematic illustration of the formation procedure of hierarchical β-Mo_2C nanotubes. Stage I: growth of Mo-polydopamine hybrid nanosheets on the pre-synthesized MoO_3 nanorods. Stage II: further growth of nanosheets and simultaneous dissolution of the MoO_3 nanorods. Stage III: formation of hierarchical β-Mo_2C nanotubes by annealing the Mo-polydopamine nanotubes.

exhibit excellent electrocatalytic performance for HER in both acidic and alkaline conditions.

The typical preparation procedure of the hierarchical β-Mo_2C nanotubes is schematically described in Figure 1. Mo-polydopamine hybrid nanotubes constructed by 2D ultrathin nanosheets are first fabricated using MoO_4^{2-} as the Mo source, dopamine hydrochloride as coordination ligand, ammonia solution as the polymerization initiator, and pre-formed MoO_3 nanorods as a reactive self-degraded template as well as additional Mo supply. In Stage I, after injecting the ammonia solution into the reaction system, tiny and flexible Mo-polydopamine hybrid nanosheets are rapidly generated through polymerization of the Mo-dopamine complex, and uniformly attach to the surface of the pre-synthesized MoO_3 nanorods to produce core–shell MoO_3@Mo-polydopamine nanorods. The MoO_3 nanorods are gradually dissolved in basic condition and form soluble MoO_4^{2-}, which could also serve as a Mo source for the further growth of Mo-polydopamine nanosheets. As a result, interesting hierarchical Mo-polydopamine nanotubes, with a hollow cavity, are obtained during Stage II. Finally, the as-prepared Mo-polydopamine nanotubes are directly annealed at 750 °C for 16 h in N_2 gas flow to produce well-crystalline β-Mo_2C hierarchical nanotubes (Stage III). During the annealing process, an in situ carburization reaction takes place between the strongly coupled Mo-based components and carbonaceous species derived from polydopamine, which forms uniform β-Mo_2C nanocrystallites embedded in a carbon matrix.

High-quality MoO_3 nanorods with a rectangle-like cross section are prepared via a facile and scalable hydrothermal method.[35] Typical field-emission scanning electron microscopy (FESEM) and transmission electron microscopy (TEM) images show that the as-prepared MoO_3 nanorods have an average width of about 200 nm and a very smooth surface (Figure S1, in the Supporting Information) with very high crystallinity (Figure S2). Employing the pre-synthesized MoO_3 nanorods as self-degradable templates, hierarchical Mo-polydopamine nanotubes could be easily obtained after reaction for 120 min under ambient conditions (Figure S3). The powder X-ray diffraction (XRD) pattern of the as-prepared Mo-polydopamine precursor (Figure S4) indicates an unknown phase with several strong diffraction peaks before 30°. This unknown phase is believed to be a Mo-containing compound with a laminar structure, which facilitates the formation of a sheet-like morphology. Indeed, Mo-polydopamine nanoflowers assembled from nanosheets can also be produced in the absence of MoO_3 nanorods, however, without any well-controlled hierarchical architecture (Figure S5).

To study the formation process of Mo-polydopamine hybrid nanotubes, TEM (Figure 2), and XRD (Figure S6) analyses are used to monitor the morphological and structural evolution as a function of the reaction time. The pristine MoO_3 nanorods have a smooth surface before the reaction (Figure 2a). At a short reaction time of 0.5 min, the rapidly formed Mo-polydopamine nanosheets are uniformly deposited on the surface of the MoO_3 nanorods (Figure 2b). Increasing the reaction time to 3 min, the MoO_3 nanorods are partially dissolved to form soluble MoO_4^{2-},[36] accompanied by the growth of Mo-polydopamine nanosheets in both thickness and size (Figure 2c). Eventually, hierarchical Mo-polydopamine nanotubes are produced after complete dissolution of the MoO_3 nanorods at a reaction time of 120 min (Figure 2d). During the reaction, the phase transformation from MoO_3 to Mo-polydopamine is confirmed by XRD measurements (Figure S6). The formation process of the hierarchical Mo-polydopamine nanotubes is based on an interesting template-engaged process, where the MoO_3 nanorods not only act as the self-degradable template but also provide an additional Mo source for the continuous growth of the Mo-polydopamine nanosheets.

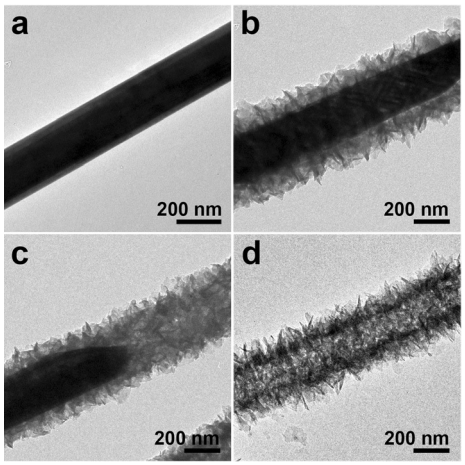

Figure 2. Typical TEM images of products after reaction for a) 0 min, b) 0.5 min, c) 3 min, and d) 120 min.

After annealing the Mo-polydopamine nanotubes in an N_2 atmosphere at 750 °C for 16 h, well-crystalline hierarchical β-Mo_2C nanotubes are obtained (Figure S7). Most of the diffraction peaks in the XRD pattern (Figure S8a) can be readily indexed to the β-Mo_2C phase with a hexagonal structure (JCPDS card no. 35-0787), which is the most active phase for HER electrocatalysts of the four phases of molybdenum carbide (α-MoC_{1-x}, β-MoC, γ-MoC, and β-Mo_2C).[20,37] The remaining two board peaks located at about 26° and 42° could be ascribed to the formation of partially

graphitic carbon derived from the organic precursor.[38] To characterize the carbon component, the Raman spectrum of the sample was measured (Figure S8b). Two distinct peaks are observed at about 1350 and 1590 cm^{-1}, corresponding to the D and G band of graphitic carbon, respectively. The intensity ratio of D band to G band, I_D/I_G, is about one, suggesting that the carbon component in the product is rather disordered with many defects. The carbon content in the product is calculated to be about 50.4 wt% from the thermogravimetric analysis (TGA) curve (Figure S9).

The morphology and structure of the hierarchical β-Mo_2C nanotubes are further investigated by FESEM and TEM. As depicted in Figure 3a, the hollow interior could be directly

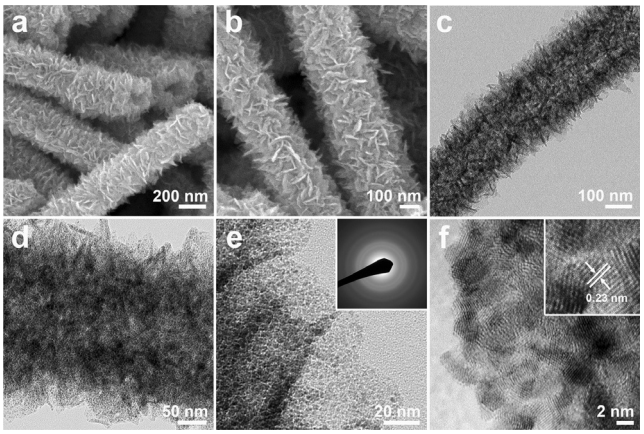

Figure 3. a,b) FESEM images, c–e) TEM, and f) HRTEM images (inset of (e): SAED pattern) of the hierarchical β-Mo_2C nanotubes (inset of (f): magnified lattice fringes).

observed from some cracked nanotubes. The walls of the tubular structures are randomly constructed by many 2D ultrathin nanosheets (Figure 3b). As shown in Figure 3c, the hierarchical β-Mo_2C nanotubes with a wall thickness of about 90 nm and a well-defined hollow interior could be clearly observed. A closer examination reveals the highly porous texture throughout the whole nanotubes (Figure 3d). The thickness of the nanosheets is measured to be about 4 nm. Interestingly, the ultrathin nanosheets are composed of numerous nanocrystallites with a small size of less than 3 nm, uniformly embedded in the continuous carbon matrix, as depicted in Figure 3e and 3f. The polycrystalline nature of the nanosheets is further confirmed by the selected area electron diffraction (SAED) pattern as shown in the inset of Figure 3e. It is worth mentioning that the in situ and confined carburization reaction prohibits the excess growth of crystallites and produces very small β-Mo_2C nanocrystallites uniformly dispersed in the simultaneously generated carbon matrix. A representative high-resolution TEM (HRTEM) image (Figure 3f) clearly shows the lattice fringes with an interplanar spacing of 0.23 nm, corresponding to the (101) planes of β-Mo_2C. Such hierarchical hollow structures offer a high Brunauer–Emmett–Teller (BET) surface area of 127 $m^2 g^{-1}$ (Figure S10), which is beneficial for their application in electrocatalysis.

The as-prepared hierarchical β-Mo_2C nanotubes are evaluated as an electrocatalyst for hydrogen evolution reaction (HER) in both acidic and alkaline conditions. The hierarchical β-Mo_2C nanotubes exhibit optimal performance with a loading mass on the glass carbon (GC) disk electrode of 0.75 mg cm^{-2} (Figure S12). Figure 4a shows the HER polarization curves of hierarchical β-Mo_2C nanotubes based on electrodes in 0.5 M H_2SO_4 and 0.1 M KOH. The current corresponding to electrochemical hydrogen evolution increases rapidly starting from small overpotentials, which verify the high catalytic activity of the as-prepared β-Mo_2C nanotubes towards HER in both acidic and alkaline conditions. From the low current density region of the Tafel plots where the current response deviates from the linear region (Figure S13), the onset potentials of the hierarchical β-Mo_2C nanotubes are estimated to be about −82 mV and −37 mV in

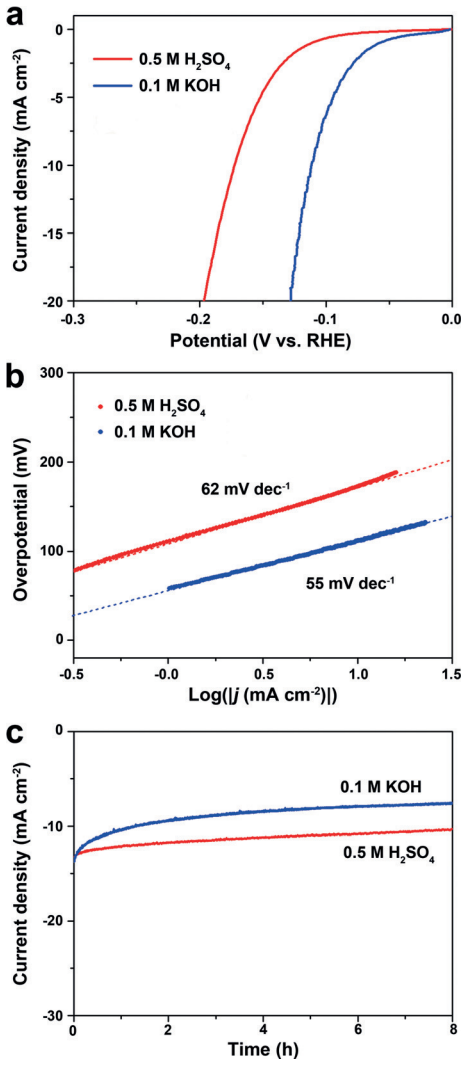

Figure 4. Electrochemical evaluation of hierarchical β-Mo_2C nanotubes in 0.5 M H_2SO_4 (red line) and 0.1 M KOH (blue line). a) Polarization curves (iR corrected) on the GC electrode at 2 $mV s^{-1}$, b) Tafel slopes, and c) time-dependent current density curves under $\eta = 170$ mV in 0.5 M H_2SO_4 and $\eta = 120$ mV in 0.1 M KOH.

0.5 M H_2SO_4 and 0.1 M KOH, respectively. In 0.5 M H_2SO_4, overpotentials of 172 mV and 197 mV can lead to current densities of 10 mA cm^{-2} and 20 mA cm^{-2}, respectively, which is superior to the β-Mo_2C nanoflowers (Figure S14). While much smaller overpotentials of 112 and 127 mV are required for the hierarchical β-Mo_2C nanotubes to drive current densities of 10 and 20 mA cm^{-2} respectively in 0.1 M KOH. Moreover, the exchange current densities of the hierarchical β-Mo_2C nanotubes are 0.017 mA cm^{-2} in 0.5 M H_2SO_4 and 0.087 mA cm^{-2} in 0.1 M KOH. The linear portions of the Tafel plots (Figure 4b) are fitted to the Tafel equation ($\eta = b\log j +$ a, where j is the current density and b is the Tafel slope), yielding Tafel slopes of approximately 62 and 55 mV decade^{-1} in 0.5 M H_2SO_4 and 0.1 M KOH, respectively. The values of the Tafel slopes suggest that the hydrogen evolution might be based on the Volmer–Heyrovsky mechanism.[5,22] The electrocatalytic activity of the hierarchical β-Mo_2C nanotubes for HER is considered good among the noble metal-free electrocatalysts, especially considering the versatility to operate in both acidic and basic solutions (Table S1 and S2). The higher HER activity of hierarchical β-Mo_2C nanotubes in basic solution is consistent with literature reports,[20,23] and might be related to the different reaction mechanisms and reaction species involved.

To evaluate the stability of the hierarchical β-Mo_2C nanotubes, the electrode is operated at certain potentials to obtain the time-dependent current (Figure 4c). There is some minor current drop at the beginning of the potentiostatic measurements, and the current gradually stabilizes afterwards, which demonstrates the good stability of the hierarchical β-Mo_2C nanotubes during the HER process. In particular, the stability in acidic solution is better than that in basic solution, which might be related to the corrosion of carbon by alkaline. Such electrochemical stability of the hierarchical β-Mo_2C nanotubes is also verified by the drift of the polarization curves under repeated potential sweeps (Figure S15).

Such high electrocatalytic HER performance can be ascribed to the following factors: 1) ultra-small β-Mo_2C nanocrystallites uniformly distributed on highly conductive carbon nanosheets enable the full utilization of active sites of catalyst and rapid transport of electrons; 2) the highly porous hierarchical hollow structure would enlarge the contact surface between electrode and electrolyte, and facilitate the charge and mass transfer during the electrochemical reactions; 3) the unique one-dimensional nanostructures would provide a continuous and effective conducting network in micrometer scale; 4) good robustness of the hierarchical structures guarantees high stability of the electrocatalyst during long-term operation.

In summary, we report a novel strategy to synthesize hierarchical β-Mo_2C nanotubes organized by 2D ultrathin nanosheets as an excellent electrocatalyst for electrochemical hydrogen evolution. Mo-polydopamine hybrid nanotubes are first synthesized via a facile template-engaged approach by using MoO_3 nanorods as both template and additional Mo source along with the in situ polymerization of dopamine. The hierarchical β-Mo_2C nanotubes are obtained by directly carburizing the Mo-polydopamine nanotubes under an inert atmosphere. The well-defined tubular structure, ultrathin nanosheet building blocks, and ultra-small primary Mo_2C nanocrystallites give rise to many appealing features, especially a large exposed active surface and improved charge transport. By virtue of the unique structural advantages, the as-prepared hierarchical β-Mo_2C nanotubes demonstrate excellent electrocatalytic performance for hydrogen evolution in both acidic and alkaline conditions, with small over potential and high stability.

Keywords: electrocatalysis · hydrogen evolution reaction · molybdenum carbide · nanosheets · nanotubes

How to cite: *Angew. Chem. Int. Ed.* **2015**, *54*, 15395–15399
Angew. Chem. **2015**, *127*, 15615–15619

[1] L. Schlapbach, A. Zuttel, *Nature* **2001**, *414*, 353.
[2] J. A. Turner, *Science* **2004**, *305*, 972.
[3] M. S. Dresselhaus, I. L. Thomas, *Nature* **2001**, *414*, 332.
[4] X. Zou, Y. Zhang, *Chem. Soc. Rev.* **2015**, *44*, 5148.
[5] C. G. Morales-Guio, L. A. Stern, X. Hu, *Chem. Soc. Rev.* **2014**, *43*, 6555.
[6] J. Greeley, T. F. Jaramillo, J. Bonde, I. B. Chorkendorff, J. K. Norskov, *Nat. Mater.* **2006**, *5*, 909.
[7] M. G. Walter, E. L. Warren, J. R. McKone, S. W. Boettcher, Q. Mi, E. A. Santori, N. S. Lewis, *Chem. Rev.* **2010**, *110*, 6446.
[8] Z. Xing, Q. Liu, A. M. Asiri, X. Sun, *Adv. Mater.* **2014**, *26*, 5702.
[9] Q. Lu, G. S. Hutchings, W. Yu, Y. Zhou, R. V. Forest, R. Tao, J. Rosen, B. T. Yonemoto, Z. Cao, H. Zheng, J. Q. Xiao, F. Jiao, J. G. Chen, *Nat. Commun.* **2015**, *6*, 6567.
[10] E. J. Popczun, C. G. Read, C. W. Roske, N. S. Lewis, R. E. Schaak, *Angew. Chem. Int. Ed.* **2014**, *53*, 5427; *Angew. Chem.* **2014**, *126*, 5531.
[11] J. Tian, Q. Liu, N. Cheng, A. M. Asiri, X. Sun, *Angew. Chem. Int. Ed.* **2014**, *53*, 9577; *Angew. Chem.* **2014**, *126*, 9731.
[12] Y. Zhao, F. Zhao, X. Wang, C. Xu, Z. Zhang, G. Shi, L. Qu, *Angew. Chem. Int. Ed.* **2014**, *53*, 13934; *Angew. Chem.* **2014**, *126*, 14154.
[13] J. Xie, S. Li, X. Zhang, J. Zhang, R. Wang, H. Zhang, B. Pan, Y. Xie, *Chem. Sci.* **2014**, *5*, 4615.
[14] X. Zou, X. Huang, A. Goswami, R. Silva, B. R. Sathe, E. Mikmekova, T. Asefa, *Angew. Chem. Int. Ed.* **2014**, *53*, 4372; *Angew. Chem.* **2014**, *126*, 4461.
[15] D. Kong, H. Wang, J. J. Cha, M. Pasta, K. J. Koski, J. Yao, Y. Cui, *Nano Lett.* **2013**, *13*, 1341.
[16] M. R. Gao, J. X. Liang, Y. R. Zheng, Y. F. Xu, J. Jiang, Q. Gao, J. Li, S. H. Yu, *Nat. Commun.* **2015**, *6*, 5982.
[17] M. Gong, W. Zhou, M. C. Tsai, J. Zhou, M. Guan, M. C. Lin, B. Zhang, Y. Hu, D. Y. Wang, J. Yang, S. J. Pennycook, B. J. Hwang, H. Dai, *Nat. Commun.* **2014**, *5*, 4695.
[18] R. Wu, J. Zhang, Y. Shi, D. Liu, B. Zhang, *J. Am. Chem. Soc.* **2015**, *137*, 6983.
[19] Y. Zheng, Y. Jiao, Y. Zhu, L. H. Li, Y. Han, Y. Chen, A. Du, M. Jaroniec, S. Z. Qiao, *Nat. Commun.* **2014**, *5*, 3783.
[20] H. Vrubel, X. Hu, *Angew. Chem. Int. Ed.* **2012**, *51*, 12703; *Angew. Chem.* **2012**, *124*, 12875.
[21] P. Xiao, X. Ge, H. Wang, Z. Liu, A. Fisher, X. Wang, *Adv. Funct. Mater.* **2015**, *25*, 1520.
[22] L. Liao, S. Wang, J. Xiao, X. Bian, Y. Zhang, M. D. Scanlon, X. Hu, Y. Tang, B. Liu, H. H. Girault, *Energy Environ. Sci.* **2014**, *7*, 387.
[23] H. B. Wu, B. Y. Xia, L. Yu, X. Y. Yu, X. W. Lou, *Nat. Commun.* **2015**, *6*, 6512.
[24] Y. Liu, K. Ai, L. Lu, *Chem. Rev.* **2014**, *114*, 5057.
[25] Q. Ye, F. Zhou, W. Liu, *Chem. Soc. Rev.* **2011**, *40*, 4244.

[26] H. Lee, S. M. Dellatore, W. M. Miller, P. B. Messersmith, *Science* **2007**, *318*, 426.
[27] C. Zhao, J. Kong, L. Yang, X. Yao, S. L. Phua, X. Lu, *Chem. Commun.* **2014**, *50*, 9672.
[28] K. Gilbert, K. Kustin, *J. Am. Chem. Soc.* **1976**, *98*, 5502.
[29] J. Liu, X. W. Liu, *Adv. Mater.* **2012**, *24*, 4097.
[30] X. Zhuang, Y. Mai, D. Wu, F. Zhang, X. Feng, *Adv. Mater.* **2015**, *27*, 403.
[31] H. Tang, C. M. Hessel, J. Wang, N. Yang, R. Yu, H. Zhao, D. Wang, *Chem. Soc. Rev.* **2014**, *43*, 4281.
[32] X. Y. Yu, H. Hu, Y. Wang, H. Chen, X. W. Lou, *Angew. Chem. Int. Ed.* **2015**, *54*, 7395; *Angew. Chem.* **2015**, *127*, 7503.
[33] F. X. Ma, H. Hu, H. B. Wu, C. Y. Xu, Z. Xu, L. Zhen, X. W. Lou, *Adv. Mater.* **2015**, *27*, 4097.
[34] J. Qi, X. Lai, J. Wang, H. Tang, H. Ren, Y. Yang, Q. Jin, L. Zhang, R. Yu, G. Ma, Z. Su, H. Zhao, D. Wang, *Chem. Soc. Rev.* **2015**, *44*, 6749.
[35] J. S. Chen, Y. L. Cheah, S. Madhavi, X. W. Lou, *J. Phys. Chem. C* **2010**, *114*, 8675.
[36] F. Han, L. Ma, Q. Sun, C. Lei, A. Lu, *Nano Res.* **2014**, *7*, 1706.
[37] C. Wan, Y. N. Regmi, B. M. Leonard, *Angew. Chem. Int. Ed.* **2014**, *53*, 6407; *Angew. Chem.* **2014**, *126*, 6525.
[38] W. Cui, N. Cheng, Q. Liu, C. Ge, A. M. Asiri, X. Sun, *ACS Catal.* **2014**, *4*, 2658.

Received: September 17, 2015
Published online: November 3, 2015

